



RESEARCH ARTICLE

Hip joint center lateralization minimally affects the biomechanics of patient-specific flanged acetabular components: A computational model

Haena-Young Lee¹  | Friedrich Boettner² | Jason L. Blevins² |
Jose A. Rodriguez² | Joseph D. Lipman¹ | Fernando J. Quevedo González¹  |
Mathias P. Bostrom² | Timothy M. Wright¹ | Peter K. Sculco²

¹Department of Biomechanics, Hospital for Special Surgery, New York, New York, USA

²Stavros Niarchos Foundation Complex Joint Reconstruction Center, Hospital for Special Surgery, New York, New York, USA

Correspondence

Haena-Young Lee, Department of Biomechanics, Hospital for Special Surgery, 535 East 70th St, New York, NY 10021, USA.
Email: leeha@hss.edu

Funding information

Stavros Niarchos Foundation

Abstract

Patient-specific flanged acetabular components are utilized to treat failed total hip arthroplasties with large acetabular defects. Previous clinical studies from our institution showed that these implants tend to lateralize the acetabular center of rotation. However, the clinical impact of lateralization on implant survivorship is debated. Our goal was to develop a finite element model to quantify how lateralization of the native hip center affects periprosthetic strain and implant-bone micromotion distributions in a static level gait loading condition. To build the model, we computationally created a superomedial acetabular defect in a computed tomography 3D reconstruction of a native pelvis and designed a flanged acetabular implant to address this simulated bone defect. We modeled two implants, one with ~1 cm and a second with ~2 cm of hip center lateralization. We applied the maximum hip contact force and corresponding abductor force observed during level gait. The resulting strains were compared to bone fatigue strength (0.3% strain) and the micromotions were compared to the threshold for bone ingrowth (20 µm). Overall, the model demonstrated that the additional lateralization only slightly increased the area of bone at risk of failure and decreased the areas compatible with bone ingrowth. This computational study of patient-specific acetabular implants establishes the utility of our modeling approach. Further refinement will yield a model that can explore a multitude of variables and could be used to develop a biomechanically-based acetabular bone loss classification system to guide the development of patient-specific implants in the treatment of large acetabular bone defects.

KEYWORDS

acetabular bone loss, biomechanics, finite element modeling, hip, revision total hip arthroplasty

1 | INTRODUCTION

One of the most difficult aspects of revision total hip arthroplasty (THA) is the management of severe acetabular bone loss.¹ Complex acetabular bone defects cannot always be adequately addressed by

standard implant designs.² Patient-specific flanged acetabular components (FACs) are particularly useful for defects with large deficiencies in the acetabular rim combined with superomedial migration of the femoral head. FACs consist of a hemispherical cup within the defect and rigid flanges that span the ilium, ischium, and

occasionally pubis, and are fixed to the bone with multiple screws (Figure 1).

Several studies have reported the clinical results of FACs in acetabular revision.³⁻⁵ In 2016, Barlow et al. conducted a retrospective review of 63 patients who had undergone revision THAs with FACs performed at our institution.⁶ FACs tended to lateralize the native hip center around 1 cm (mean 9.86 ± 11.89 mm), but in a subset of FACs that failed secondary to aseptic loosening, the construct lateralization was nearly 2 cm (18.29 ± 11.90 mm). In 2019, Jones et al. conducted a subsequent study with a larger cohort of 91 patients and found that more distal and robust ischial screw fixation was associated with improved FAC survivorship.⁷ These studies suggest that certain biomechanical variables impact FAC clinical survivorship. However, no study to date has utilized computational modeling to quantify the impact of these variables.

The purpose of this study was to computationally analyze how an additional 10 mm of hip center lateralization affects the biomechanics of patient-specific FACs. We calculated the biomechanical implant environment with two outcomes: bone strains around the FAC and micromotion between the FAC and the surrounding bone. Based on our prior clinical study, we examined these outcomes for two configurations of hip center lateralization (9.7 mm and 19.7 mm) during a static representation of level gait. We hypothesized that greater lateralization would increase areas of bone with large strains and decrease areas with small micromotion. We analyzed our results to quantify the impact of additional hip center lateralization on FAC biomechanics.

2 | METHODS

We developed the computational model for our study in four steps: (1) obtain the geometry and material properties for a native pelvis, (2) create an acetabular defect, (3) design and place a patient-specific FAC to treat the defect, and (4) perform finite element (FE) simulations to compute and analyze our primary outcomes.

2.1 | Native pelvic geometry and material properties

We selected a representative 54 year old female patient with osteoarthritis who had undergone a staged bilateral THA performed with robotic guidance.⁸ The preoperative computed tomography (CT) scan allowed us to obtain the geometry and material properties of the native hip without the presence of metal artifacts.

2.2 | Acetabular defect geometry

To create a "common" acetabular defect that would be treated with a FAC, we reviewed the radiographs and CT scans of all patients (e.g., Figure 2) from the Barlow et al. study.⁶ The consensus of the orthopedic surgeon co-authors (FB, JB, JR, MB, and PS) led to the creation of an "up and in" superomedial defect with anterior column and medial wall deficiency but an intact posterior column. To create the defect in our model, we first placed a 54 mm sphere at the center of the acetabulum. We moved the sphere medially 15 mm and superiorly 15 mm, removing any overlapping bone, to represent superomedial bone loss (Figure 3). This geometry is representative of a Paprosky 2 A acetabular defect (up and in migration, less than 3 cm of superior femoral head migration). We also removed 3 mm of bone in each anterior-posterior direction to simulate continued acetabular motion in-situ. We used Geomagic Design X (3D Systems) to perform these operations.

2.3 | Patient-specific FAC

We designed the FAC implant (Figure 4) for this created acetabular defect. The implant configuration was based on guidelines derived from previous patient-specific FACs designed and implanted at our institution. For instance, the new hip center was positioned to best reconstruct the native hip center. Ideally, restoring the hip center would require minimal additional bone removal and would not

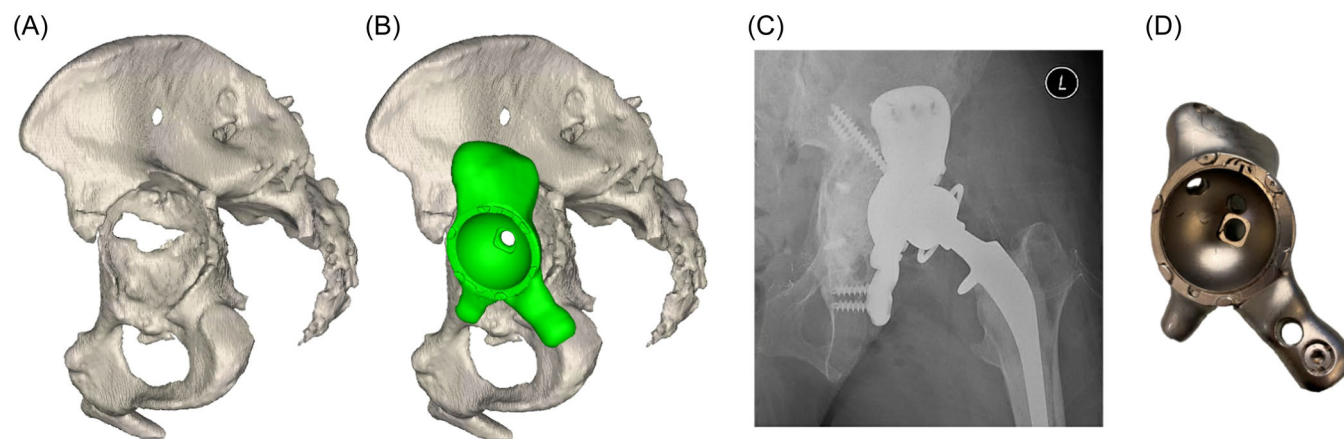


FIGURE 1 A revision THA with FAC patient case, performed at our institution. (A) 3D reconstruction of the defect hip geometry, (B) bone and implant, (C) postoperative radiograph (cropped to show the FAC), (D) retrieved implant.

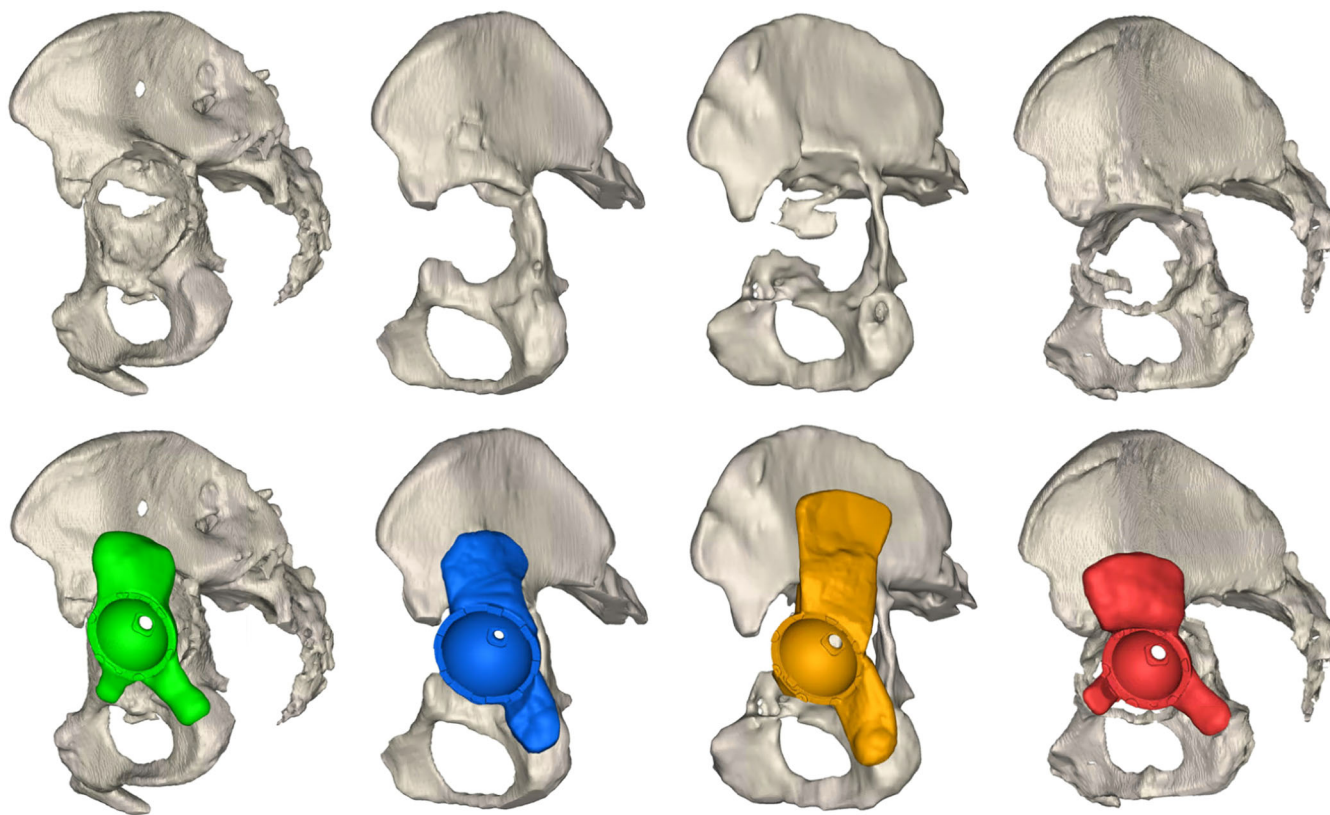


FIGURE 2 Example cohort of patients reviewed to determine characteristics of the acetabular defect to model. Common characteristics included superomedial bone loss, an intact posterior wall, and loss of the anterior column and acetabular rim.

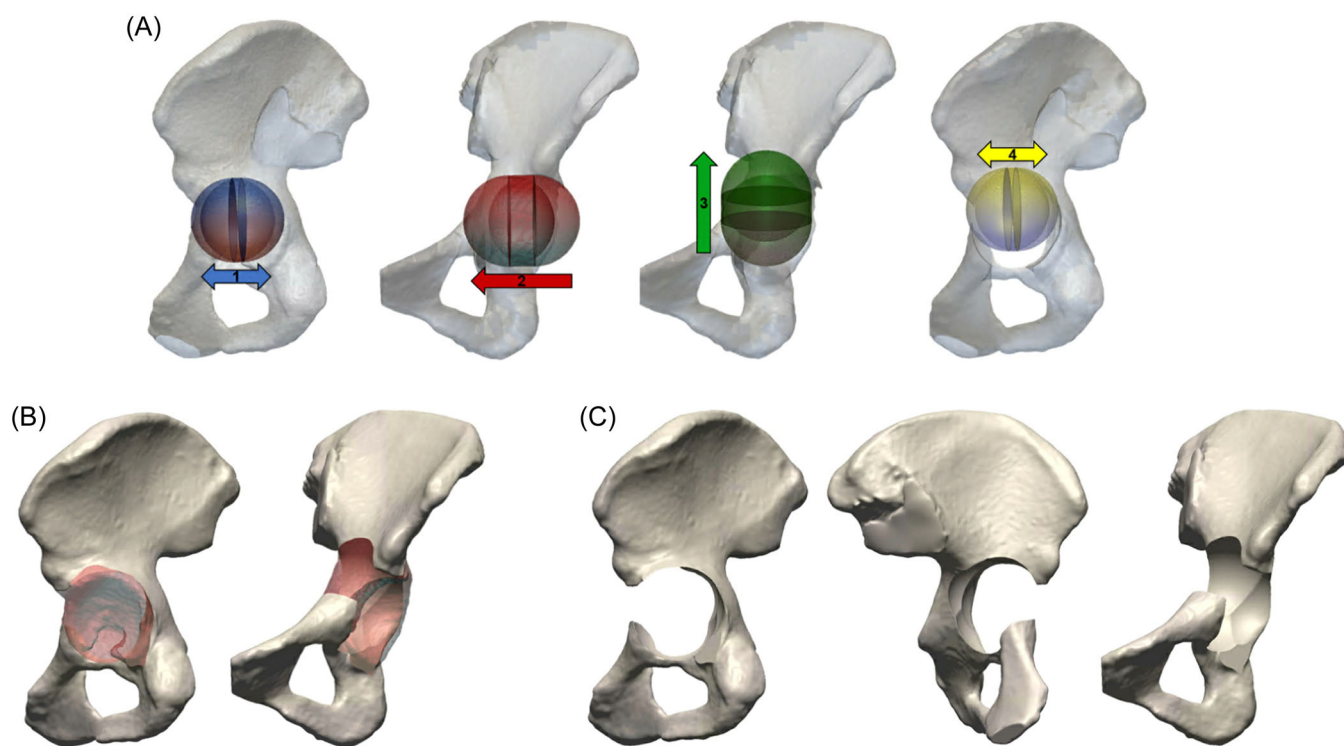


FIGURE 3 Creation of the superomedial defect model in the representative hip. (A) Translation of a 54 mm spherical tool to remove bone in the preoperative hip, 1: 3 mm each anteriorly and posteriorly, 2: 15 mm medially, 3: 15 mm superiorly, and 4: 3 mm each anteriorly and posteriorly; (B) overlay of the preoperative hip and the defect model with the removed bone in red; (C) the final defect model.

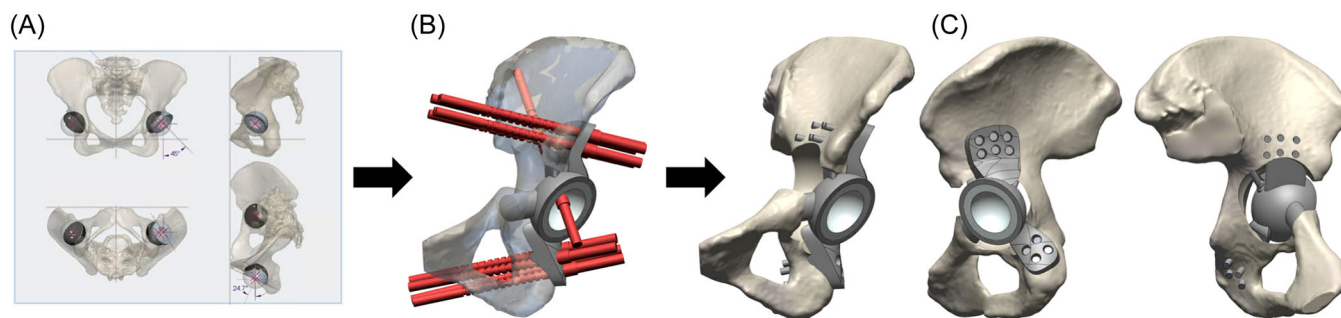


FIGURE 4 Design and placement of the FAC for the defect model. (A) Implant positioned in 45° inclination and 25° anteversion, (B) divergent screw trajectories, and (C) final defect model with FAC and screws.

lengthen the leg more than 20 mm due to risk of acute lengthening and sciatic nerve traction injury.

Additionally, the cup position is usually targeted for 45° of inclination and 25° of anteversion relative to the anterior pelvic plane, as defined by anatomic landmarks from the preoperative CT scan. A 54 mm diameter cup is typically selected because it usually fills the acetabular defect and offers the most liner options (including neutral, elevated, and constrained liners) from our most frequently used manufacturer. The iliac flange usually contains five to seven screws in two rows immediately superior to the cup and placed in the iliac wing. The ischial flange contains three to four screws that are placed in two rows of divergent trajectories in the ischial tuberosity. The dome screw is placed through the dome of the cup into the posterior column. Screws are positioned to facilitate bi-cortical contact through the best quality bone. An ilial “buttress” feature is typically designed for contact with the superior bone to assist with transfer of compressive loads into the ilium. A pubic buttress has also historically been designed, but has been omitted in the more recent FAC designs at our institution. Other implant details, such as shell and flange thickness or the minimum distance between screws, are determined by the design requirements of the manufacturer.

For this bone defect, we developed a FAC with a 54 mm cup that was 4 mm thick and was placed in 45° of inclination and 25° of anteversion. The iliac and ischial flanges were 7 mm thick and the construct contained six iliac, four ischial, and one dome screw. These screws were computationally represented as simple cylindrical posts with spherical heads and no threads. We included both ilial and pubic buttress features. We placed the implant in the defect with host bone contact with the flanges and the designated implant center of rotation 9.7 mm lateral to the native hip center.⁶ We also created a second FAC model with 19.7 mm of lateralization to observe the effects of an additional 10 mm of hip center lateralization. Both configurations had the same contact between the flanges and the bone.

2.4 | Finite element modeling

We used Abaqus (Dassault Systèmes, Vélizy-Villacoublay) to build the FE model. Based on previous studies,^{9–12} we created a mesh of 1 mm

linear tetrahedral elements, with larger 2.5 mm elements around the sacroiliac joint and pubic symphysis. The final model had over 2.1 million elements. The bone was modeled as a linear elastic, isotropic, and nonhomogeneous material. We utilized previously published methodologies¹³ to derive the nonhomogeneous elastic moduli (E) of the bone from the Hounsfield units in the preoperative CT scan of the native pelvis used in this model. The implant components were modeled as linear elastic, isotropic, and homogeneous materials. The FAC implant and screws were assigned Ti6Al4V alloy properties (E = 114 GPa, Poisson's ratio ν = 0.33) and the liner was assigned ultrahigh molecular-weight polyethylene properties (E = 646 GPa, ν = 0.4). We assumed line-to-line contact between the FAC and pelvis with an interfacial friction coefficient of 0.6. We tied the liner with the cup and modeled the screws as perfect fixation without motion between the implant and bone.

We chose to model level gait as the most common and clinically relevant loading condition. We applied two forces to the model: the hip joint contact force and the corresponding abductor force. We utilized level gait data from OrthoLoad, a public database of recorded forces in the hip joint obtained from patients with instrumented total hip implants.¹⁴ We considered the single point in time corresponding to the maximum force during level gait, which occurred at heel strike (15% of the gait cycle). In our model, we oriented the pelvis and femur to correspond to the relative position of each at heel strike.

We calculated a free body diagram to obtain the hip contact and abductor forces (Figure 5). We simplified the abductor muscles to the gluteus medius and determined its attachment footprint on the superior rim of the ilium and on the greater trochanter.^{15,16} We also assumed that the abductor line of action was at the center of the footprint and set the bodyweight force as 3/5 of the bodyweight of our 54 year old patient (66.7 kg). For level gait, the magnitude of the hip contact force was 1663 N. The magnitudes of the abductor force were 1266 N for 9.7 and 2275 N for 19.7 mm of lateralization. The abductor force increases with greater hip center lateralization due to a shorter abductor lever arm that requires more force to counteract the bodyweight force.

We validated the magnitude and direction of the forces by comparing them to those obtained from the OrthoLoad data. We transformed the hip contact force from the OrthoLoad reference

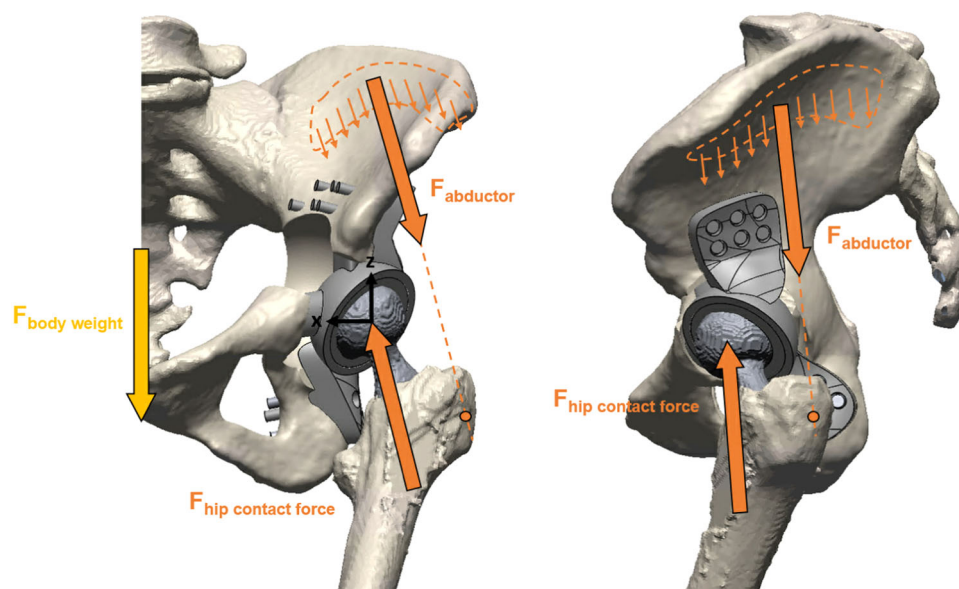


FIGURE 5 Free body diagram solved to obtain the hip contact and abductor forces for the created defect hip geometry. The relative positions of the pelvis and femur, as pictured here, correspond to those at the time point of maximum hip contact force during level gait. The sacroiliac joint and pubic symphysis were fixed; the medial cutoff line is shown here to provide a fuller anatomic picture of the model.

frame to that of our model (file pflwn1). We scaled the force from the bodyweight of the patient in OrthoLoad (99.9 kg) to that of our patient (66.7 kg). The resulting maximum hip joint contact force was 1530 N, indicating a small discrepancy of approximately two tenths of bodyweight from the previously calculated force of 1663 N. Despite the differences in patient geometries and simplification of the muscle forces, the magnitudes and directions of the forces from the free body diagram were similar to those from OrthoLoad.

We applied the maximum hip contact force of 1663 N at the center of the cup and distributed the calculated abductor muscle force across the muscle attachment footprint along the superior region of the ilium. We fixed the pelvis at the sacroiliac joint and pubic symphysis for the boundary conditions.

2.5 | Primary outcomes

We investigated the strain distributions around the FAC to analyze the mechanical burden on adjacent bone and implant-bone micromotion to analyze the likelihood of bone ingrowth. From the periprosthetic strains, we computed the bone at risk of failure as any periacetabular bone that had principal strains equal to or greater than the bone fatigue strength of 0.3% strain.¹⁷ The areas of bone at risk do not necessarily mean that the bone will fail but indicate regions of high strains, emphasizing where the transferred loads are highest in the bone given the boundary conditions and loads. We chose a relatively conservative criterion to ensure distinct strain distribution patterns for this first study. The one-to-one comparisons of the model also ensure that our conclusions regarding the impact of lateralization are valid. We quantified the areas of bone at risk of

failure as percentages of each of the implant-bone contact surfaces at the ilial flange, ischial flange, iliac screws, dome screw, and ischial screws. For micromotion, we considered a conservative threshold of 20 μ m for bone ingrowth into porous or hydroxyapatite coated surfaces.¹⁸ We quantified the areas compatible with bone ingrowth as areas with less than 20 μ m of micromotion.

3 | RESULTS

3.1 | Strain distributions

At the ilial flange, the bone at risk of failure was located along the superior and anterior edges of the FAC for both lateralization configurations (Figure 6). When the FAC lateralized the native hip center by an additional 10 mm, without adjusting the position of the ilial or ischial flanges, the ilial contact areas at risk of failure increased from 25% to 31%. Areas of elevated tensile and compressive strains were present near the iliac screw holes. At the ischial flange, the bone at risk of failure was primarily located along the posterior and distal edges of the flange for both configurations. Additional lateralization slightly decreased the ischial areas of bone at risk of failure from 16% to 12%.

The bone in contact with the screws experienced similar strain distributions for both configurations (Figure 7). The strains were larger at the bone in contact with the iliac screws than at the bone in contact with the dome or ischial screws. The areas at risk of failure for the bone in contact with the iliac screws increased from 25% to 41%. These failure areas were primarily due to compression near the bone and tension along the lengths of the screw holes. At the dome screw, none of the bone was at risk of failure for both FAC

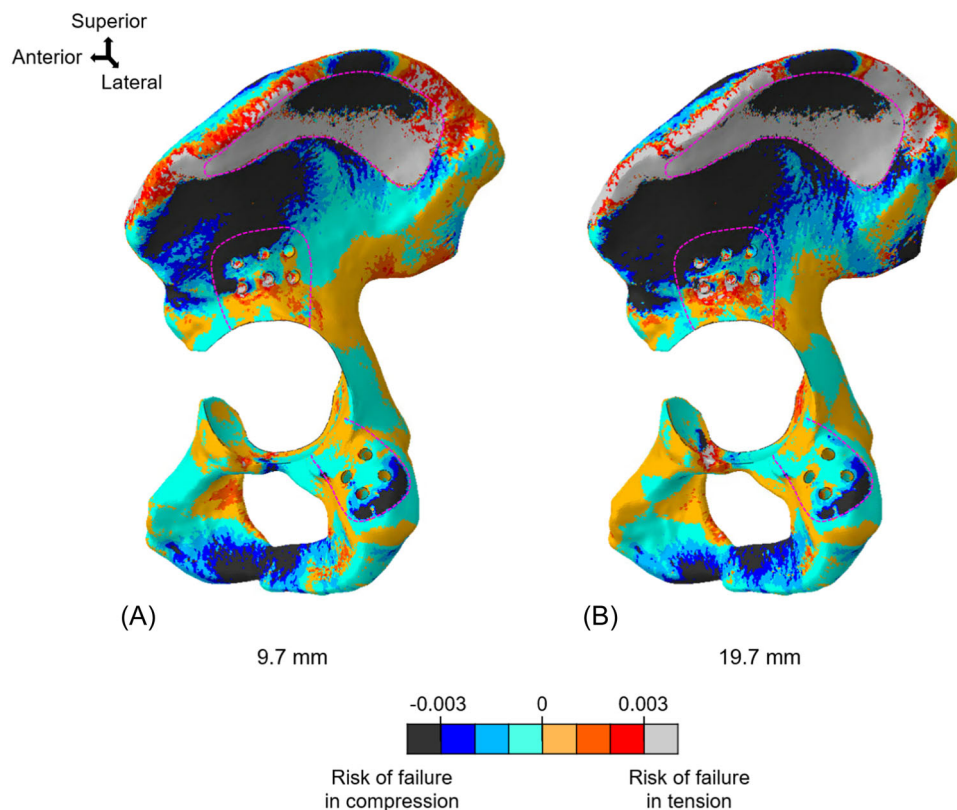


FIGURE 6 Periprosthetic strain distributions for (A) 9.7 mm and (B) 19.7 mm of hip center lateralization. The abductor surface and flanges are outlined in a dotted magenta line. Blue colors indicate bone in compression and red colors indicate bone in tension. Black and gray indicate bone with strain exceeding the bone fatigue strength in compression and tension, respectively.

configurations. At the ischial screws, the risk areas decreased from 0.5% to 0.4%, and tensile and compressive strains were elevated in the distal screws.

3.2 | Micromotion

For both FAC configurations, the micromotion at the ilial flange consisted of lift-off of the inferior aspect of the flange from the bone, indicating posterior-superior pivoting of the implant (Figure 8). At the ilial flange, the areas compatible with bone ingrowth slightly decreased with additional lateralization, from 74% to 58%. At the ischial flange, the areas compatible with bone ingrowth slightly increased, from 85% to 96%.

4 | DISCUSSION

In this computational study, we developed a FE model and applied a real-world loading condition to investigate the effects of an additional 10 mm of hip center lateralization on the biomechanics of FACs. This approach allowed us to examine the mechanics of this complex implant-bone interaction and how it relates to our two primary outcomes, periprosthetic bone strain and implant

micromotion. Bone strain reflects the mechanical burden the FAC creates in the bone. Implant-bone micromotion reflects the ability for bone ingrowth, as FACs are designed for biological fixation using backside porous or hydroxyapatite coatings. We simulated two lateralization configurations and a static loading condition of level gait. We expected that greater lateralization would result in greater areas of bone at risk and smaller areas compatible with ingrowth.

Additional hip center lateralization of 10 mm slightly increased the areas of bone adjacent to the implant at risk of failure and minimally decreased the areas where biological fixation would be likely to occur, particularly in the ilium. Overall, the area at risk for bone strain failure increased by 24% at the ilial flange, 66% at the iliac screws, and the area compatible with ingrowth decreased by 21% with additional lateralization. Interestingly, the effects on the ischium were reversed. The overall risk area decreased by 22% at the ischial flange and from 0.5% to 0.4% at the ischial screws, and the area compatible with ingrowth (micromotion below 20 μ m) actually increased by 14%. These findings suggest that the increase in magnitude of the abductor force due to the additional lateralization impacted the motion of the bone around the implant, resulting in slightly more loading on the ilium and less on the ischium. However, these percent changes are small and indicate that additional lateralization does not significantly impact FAC biomechanics. This supports the Jones et al. study from our institution, which found that hip center lateralization was not associated with

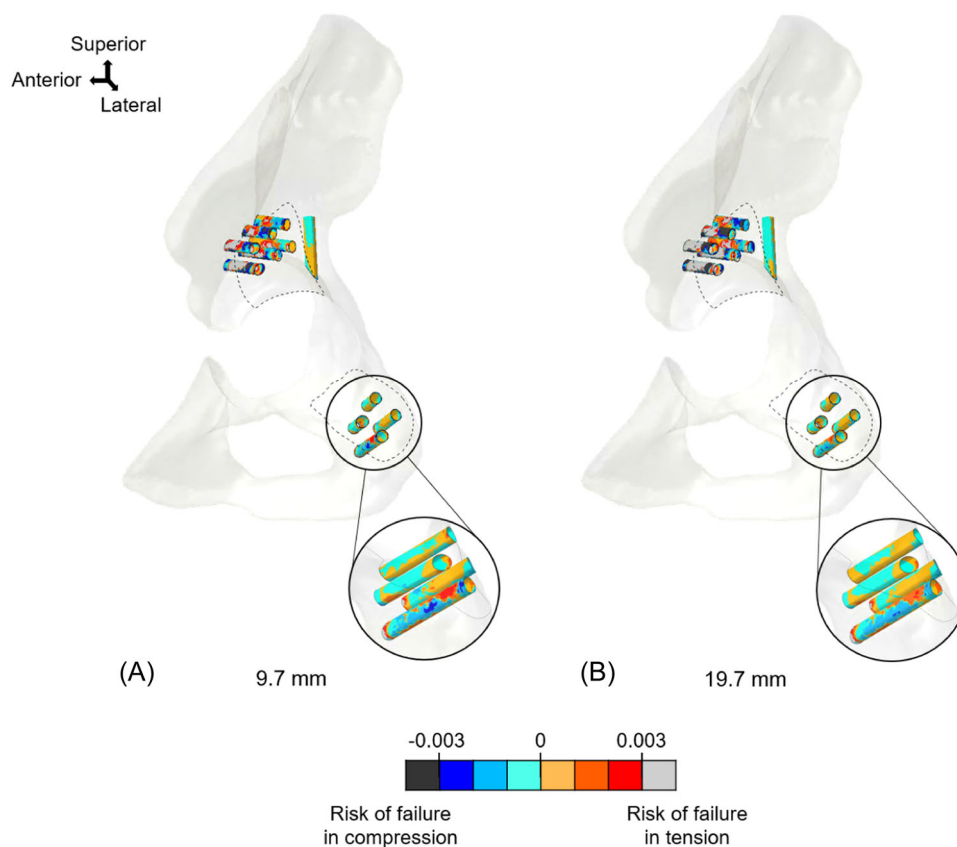


FIGURE 7 Periprosthetic strain distribution in the ilial, ischial, and dome screws for (A) 9.7 mm and (B) 19.7 mm of hip center lateralization. Blue colors indicate bone in compression and red colors indicate bone in tension. Black and gray indicate bone with strain exceeding the bone fatigue strength in compression and tension, respectively.

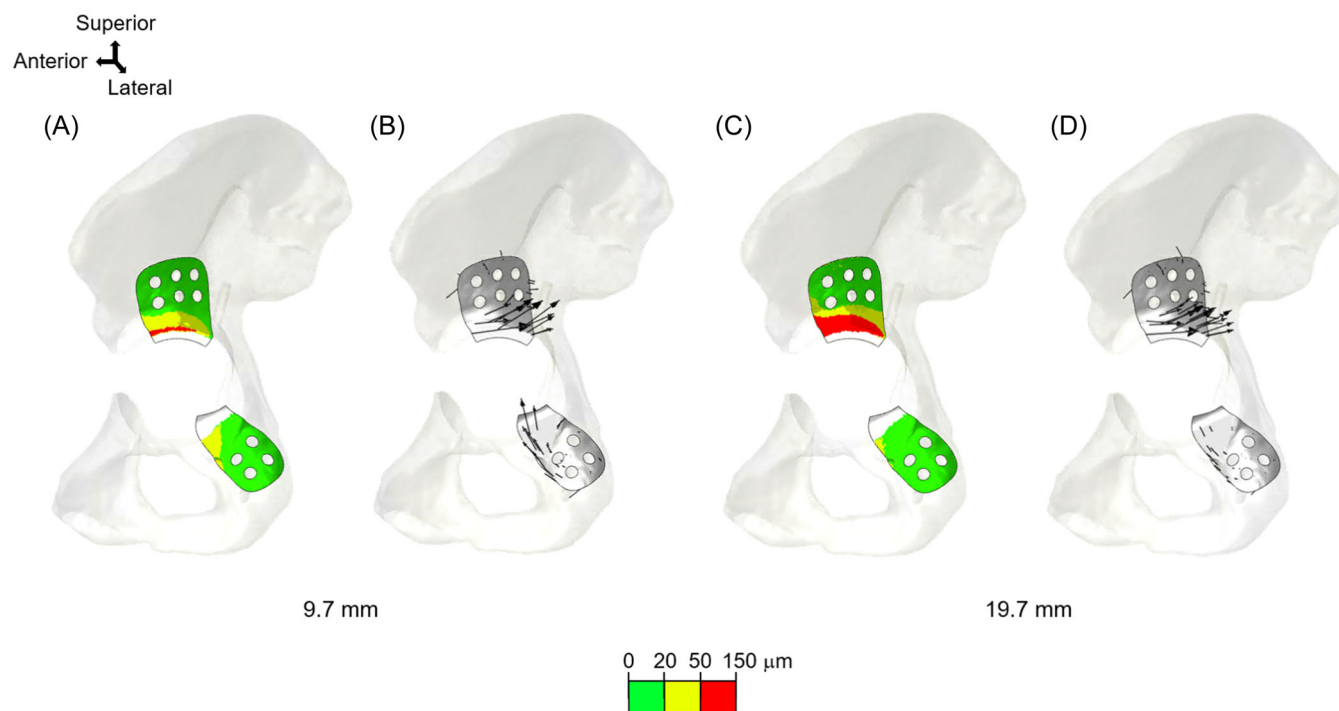


FIGURE 8 Micromotion distribution and direction at the ilial and ischial flanges for (A, B) 9.7 mm and (C, D) 19.7 mm of lateralization. Green indicates areas with micromotion less than 20 μm , the threshold for compatibility with bone ingrowth. Yellow and red indicate areas incompatible with bone ingrowth. The black arrows indicate the direction of the micromotion of the flanges relative to the bone.

inferior FAC survivorship.⁷ As found in the Barlow et al. study, the flange overlay FAC design usually requires about 1 to 2 cm of lateralization.⁶ Our results suggest that in a patient with an intact abductor, greater lateralization does not compromise implant biomechanics during level gait.

The results of the FE model demonstrate the overall deformation of the pelvis in relation to the much stiffer metallic FAC. This deformation can be seen in the compressive strains created in the bone along the edges of the flanges. The pull of the abductor along the superior rim of the ilium created tensile strain where the muscle load is applied and compressive strain on the inferior aspect of the pelvis as the iliac wing bends towards the greater trochanter. This general bending results in compressive strain along the flange edges and posterior-superior micromotion of the implant relative to the bone.

Our model has several limitations. We modeled a single defect geometry with one FAC design, so the results are not generalizable to all revision THA with FAC cases. We also used an elastic modulus distribution based on the Hounsfield units of the CT scan of a patient about to undergo primary THA. In the revision setting for which an FAC would typically be used, the bone density would likely be adversely affected, particularly in the ischium and around the acetabular defect. A model incorporating adverse ischial bone quality may show different or more drastic trends in the strain and micromotion distributions. Another limitation was the assumption of a normal abductor muscle force. The abductor muscles are often weakened in patients requiring revision surgery with an FAC. We also assumed isotropic bone properties, perfect implant-bone contact, and rigidly fixed screws with no threads. Other investigators have included similar conditions in FE models of screw fixation in complex implant-bone systems.^{19,20} Further, we simulated a static loading condition that did not account for the evolution of bone failure. Other activities such as stair ascent or rising from a chair may produce different strain and micromotion distributions. Finally, a convergence study was not performed and this model was not experimentally validated because the computational model was based on the CT scan of a living subject. Despite these limitations, a controlled environment allows us to investigate one design variable, hip center position, and its specific impact on FAC biomechanics.

We utilized computational FE modeling to demonstrate that additional lateralization of the native hip center has a relatively small impact on the risk of bone failure and excessive implant-bone micromotion in revision THAs with FACs. A significant advantage to this approach is that such an established model can be expanded upon to explore other clinical and design variables, which may have greater effects on FAC biomechanics. Encouraged by our findings and with further refinement of our model, we intend to next examine regional variations in bone quality, bone-screw interfaces, and other acetabular defect geometries.

AUTHOR CONTRIBUTIONS

Haena-Young Lee, Joseph D. Lipman, Fernando J. Quevedo González, and Timothy M. Wright contributed to project design, data collection and analysis, and writing of the manuscript. Friedrich Boettner, Jason

L. Blevins, Jose A. Rodriguez, Mathias P. Bostrom, and Peter K. Sculco contributed to project design, interpretation of data, and revision of the manuscript. All authors read and approved the final submitted manuscript.

ACKNOWLEDGMENTS

Research reported in this publication was supported by the Stavros Niarchos Complex Joint Reconstruction Center at the Hospital for Special Surgery.

CONFLICT OF INTEREST STATEMENT

The authors have no conflicts of interest.

ORCID

Haena-Young Lee  <http://orcid.org/0000-0001-9960-0310>

Fernando J. Quevedo González  <http://orcid.org/0000-0001-6521-8754>

REFERENCES

1. Sculco PK, Wright T, Malahias MA, et al. The diagnosis and treatment of acetabular bone loss in revision hip arthroplasty: an international consensus symposium. *HSS J Musculoskeletal J Hosp Special Surg*. 2022;18:8-41.
2. Mäkinen TJ, Abolghasemian M, Watts E, et al. Management of massive acetabular bone defects in revision arthroplasty of the hip using a reconstruction cage and porous metal augment. *Bone Jt J*. 2017;99-B:607-613.
3. De Martino I, Strigelli V, Cacciola G, Gu A, Bostrom MP, Sculco PK. Survivorship and clinical outcomes of custom triflange acetabular components in revision total hip arthroplasty: a systematic review. *J Arthroplasty*. 2019;34(10):2511-2518.
4. Moore KD, McClenny MD, Wills BW. Custom triflange acetabular components for large acetabular defects: minimum 10-Year follow-up. *Orthopedics*. 2018;41(3):e316-e320.
5. Gladnick BP, Fehring KA, Odum SM, Christie MJ, DeBoer DK, Fehring TK. Midterm survivorship after revision total hip arthroplasty with a custom triflange acetabular component. *J Arthroplasty*. 2018;33(2):500-504.
6. Barlow BT, Oi KK, Lee Y, Carli AV, Choi DS, Bostrom MP. Outcomes of custom flange acetabular components in revision total hip arthroplasty and predictors of failure. *J Arthroplasty*. 2016;31:1057-1064.
7. Jones CW, Choi DS, Sun P, et al. Clinical and design factors influence the survivorship of custom flange acetabular components. *Bone Jt J*. 2019;101-B(6_suppl_B):68-76.
8. Debbi EM, Quevedo González FJ, Jerabek SA, Wright TM, Vigdorichik JM. Three-dimensional functional impingement in total hip arthroplasty: a biomechanical analysis. *J Arthroplasty*. 2022;37(7):S678-S684.
9. Ricci PL, Maas S, Kelm J, Gerich T. Finite element analysis of the pelvis including gait muscle forces: An investigation into the effect of rami fractures on load transmission. *J Exp Orthop*. 2018;5(1):33.
10. Dong E, Wang L, Iqbal T, et al. Finite element analysis of the pelvis after customized prosthesis reconstruction. *J Bionic Eng*. 2018;15:443-451.
11. Fallahnezhad K, O'Rourke D, Bahl JS, Thewlis D, Taylor M. The role of muscle forces and gait cycle discretization when assessing acetabular cup primary stability: a finite element study. *Comput Methods Programs Biomed*. 2023;230:107351.

12. Coultrup OJ, Hunt C, Wroblewski BM, Taylor M. Computational assessment of the effect of polyethylene wear rate, mantle thickness, and porosity on the mechanical failure of the acetabular cement mantle. *J Orthop Res*. 2010;28:565-570.
13. Quevedo González FJ, Lipman JD, Lo D, et al. Mechanical performance of cementless total knee replacements: it is not all about the maximum loads. *J Orthop Res*. 2019;37(2):350-357.
14. Bergmann G, ed. "OrthoLoad". Charité Universitaetsmedizin Berlin; 2008.
15. Kapandji AI. The Physiology of the Joints. *The Lower Limb*. 2, 6th ed. Elsevier; 2011:323.
16. © Pharma Intelligence UK Ltd (trading as Primal Pictures), 2023. www.primalpictures.com
17. Dendorfer S, Maier HJ, Taylor D, Hammer J. Anisotropy of the fatigue behaviour of cancellous bone. *J Biomech*. 2008;41(3):636-641.
18. Jasty M, Bragdon C, Burke Dennis, et al. In vivo skeletal responses to porous-surfaced implants subjected to small induced motions. *Am J Bone Jt Surg*. 1997;79(5):707-714.
19. Varga P, Inzana JA, Fletcher JWA, et al. Cement augmentation of calcar screws may provide the greatest reduction in predicted screw cut-out risk for proximal humerus plating based on validated parametric computational modelling. *Bone Joint Res*. 2020;9(9):534-542.
20. Wang Y, Qi E, Zhang X, Xue L, Wang L, Tian J. A finite element analysis of relationship between fracture, implant and tibial tunnel. *Sci Rep*. 2021;11(1):1781.

How to cite this article: Lee H-Y, Boettner F, Blevins JL, et al. Hip joint center lateralization minimally affects the biomechanics of patient-specific flanged acetabular components: a computational model. *J Orthop Res*. 2024;1-9. [doi:10.1002/jor.25864](https://doi.org/10.1002/jor.25864)